Observation of Size-Dependent Thermalization in CdSe Nanocrystals Using Time-Resolved Photoluminescence Spectroscopy

Daniel C. Hannah, Nicholas J. Dunn, Sandrine Ithurria, Dmitri V. Talapin, Lin X. Chen, Matthew Pelton, George C. Schatz, and Richard D. Schaller

Phys. Rev. Lett. **107**, 177403 — Published 20 October 2011

DOI: 10.1103/PhysRevLett.107.177403

Size-Dependent Thermalization Dynamics in CdSe Nanocrystals

Daniel C. Hannah,[1] Nicholas J. Dunn,[1] Sandrine Ithurria,[3] Dmitri V. Talapin,[2,3] Lin X. Chen,[1,2] Matthew Pelton,[2] George C. Schatz,[1] and Richard D. Schaller[1,2*]

[1]Department of Chemistry, Northwestern University, Evanston IL 60208, [2]Center for Nanoscale Materials, Argonne National Laboratory, Argonne, IL 60439, [3]Department of Chemistry, University of Chicago, Chicago, IL 60637

*Electronic address: schaller@anl.gov

We report heat dissipation times in semiconductor nanocrystals (NCs) of CdSe. Specifically, a previously unresolved, sub-nanosecond decay component in the low-temperature photoluminescence (PL) decay dynamics exhibits longer decay lifetimes (tens to hundreds of picoseconds) for larger NCs as well as a size-independent, ~25-meV spectral shift. We attribute the fast relaxation to transient phonon-mediated relaxation arising from non-equilibrium acoustic phonons. Following acoustic phonon dissipation, the dark exciton state recombines more slowly via LO phonon assistance resulting in the observed spectral shift. The measured relaxation timescales agree with classical calculations of thermal diffusion, indicating that interface thermal conductivity does not limit thermal transport in these semiconductor NC dispersions.

Colloidal semiconductor nanocrystal (NC) quantum dots offer size-tunable band gaps, solution processing, and controllable surface functionality that can impact technologies ranging from lighting [1] and bio-labels [2] to photovoltaics [3] and thermoelectrics [4, 5]. While much of the materials community focuses on new compositions as well as determination of NC optical properties and incorporation into devices, thermal management, which is crucial to each of the highlighted technologies, will become an increasingly important factor for the use of these thermodynamically compromised materials. Measurement and manipulation of thermal outflow rates in nanoscale semiconductors at present, however, represents a challenge. Comprehensive understanding of the electron-hole pair ("exciton") dynamics, electronic structure, and thermal properties of such designer materials in aggregate is vital to their successful application.

Significant information exists for CdSe NCs regarding carrier dynamics and electronic structure, the relevant findings of which we summarize here. Following photoexcitation, excitonic intraband relaxation down to the "band-edge" states takes place on sub-picosecond to single-picosecond timescales [6-8]. Radiative recombination, on the other hand, requires tens to hundreds of nanoseconds and exhibits strong temperature dependence owing both to details of the size- and shape-specific exciton fine structure as well as exciton-phonon interactions [9-16]. Crystal field effects, spin-orbit coupling, and the electron-hole exchange interaction [11, 12] give rise to the energetic ordering and size-dependent energy spacings of the band-edge exciton states. A dipole forbidden (optically passive or "dark") lowest-energy exciton, with spin projection $J=\pm2$ along the wurtzite c-axis, resides below an optically allowed (bright, $J=\pm1$) exciton state by 2-17 meV, with larger dark-bright splittings (Δ_{db}) for smaller NC sizes [10]. At cryogenic temperatures, insufficient thermal energy exists to populate the lowest-energy bright exciton state, and microsecond lifetimes result due to the weakly emissive character of the dark exciton.

By contrast, at higher temperatures, a thermal (Boltzmann) population of bright excitons radiates with an established lifetime of ~20 ns [13]. Nirmal et al. established values of Δ_{db} from the energy difference between a spectrally narrow excitation laser and the proximal, zero-phonon PL peak position owing to spin-forbidden recombination from dark excitons [10]. The same study found LO-phonon assisted emission bands at lower energy wherein emission of a photon and generation of an LO phonon yields momentum conserving transitions from the dark state. Magnetic fields were found to quantum mechanically mix proximal bright and dark states, which increases the zero-phonon amplitude relative to the LO-phonon assisted feature and yields a notable increase in the radiative recombination rate [10]. Also, cryogenic four-wave mixing (FWM) measurements suggest that optically bright photo-excited excitons decay into lowest-energy dark exciton states roughly in the same time as intraband relaxation [17].

Here, we examine a longstanding, poorly understood feature in CdSe NC dynamics and attribute it to thermal dissipation. Specifically, in addition to the more fully characterized dark and bright radiative lifetimes, Crooker showed that low temperature time-resolved PL (trPL) measurements exhibit an unusual, rapid initial decay for sample temperatures below ~20 K, signatures of which appear in numerous reports [9, 13-16]. To date, this fast burst of PL has remained uncharacterized due to an instrumental lack of sufficient temporal resolution. We temporally and spectrally resolve this feature, revealing clear size-dependent dynamics as well as distinct spectral characteristics that, taken together in the context of literature from metals and semiconductors, permit us to assign the feature to size-dependent thermal outflow. While low temperatures are required in order to observe this outflow, the thermal transport constants may be scaled to temperatures of relevance to device applications.

We examine several sizes of CdSe NCs capped with octadecylamine, which exhibit PL quantum yields in excess of 20% at room temperature. Small discrepancies exist regarding available CdSe sizing curves (used to convert absorption maximum to NC radius), but these did not qualitatively impact presented results. NCs were dispersed in a 1:1 octadecane:eicosane solvent and dripped onto a sapphire substrate. The samples were loaded into a closed-cycle helium cryostat and photo-excited with 35 fs pulses from a 2 kHz amplified Ti-sapphire laser at 3eV. The excitation fluence utilized corresponds to the production of less than 0.05 electron-hole pairs per NC per pulse, and results were unchanged for 3x higher or lower excitation intensities. PL photons were directed to a 150 mm spectrograph and streak camera. Detector regions were binned vertically or horizontally to produce time-resolved spectra or spectrally-resolved dynamics, respectively.

A streak camera image recorded at 2.6 K [Fig. 1(a)] for the first few hundred picoseconds following photoexcitation of a 1.6-nm radius NC sample (556 nm 1S absorbance maximum) shows a fast initial burst of emission that is not observed at 80 K [Fig 1(b)], in qualitative agreement with previous reports that did not temporally or spectrally resolve this feature [13-16]. At 2.6 K, time-resolved spectra [Fig. 1(c)] exhibit shorter wavelength PL during the first ~80ps following excitation which red-shifts to a constant value for longer times, whereas the 80 K sample temperature lacks any pronounced spectral shift over the same time range. Dynamics in Figs. 1(e) and 1(f) display a fast relaxation feature at 2.6 K for bluer wavelengths that is largely absent from the redder PL at 2.6 K, and is absent for all wavelengths in the 80 K data.

Single Gaussian fits of the ensemble-broadened spectra shown in Fig. 1(c) yield similar full-width at half maximum linewidths (16.2 nm for t=0 to 20 ps and 17.3 nm for t = 320 to 340 ps), which suggests that a single population evolves to emit with reduced energy over time. For

the dynamics collected at 2.6 K in Fig. 1(e), we find that the decay on the blue side of the PL is well-described by a biexponential decay, while the redder PL dynamics at low temperature and all of the dynamics recorded at 80 K appear single exponential in the time-window examined. The biexponential fit time-constants differ by more than one order of magnitude, which allows for highly independent fits. While the spectrally resolved dynamics in Fig. 1(e) each exhibit fast decay constants that differ by ~25% for proximal spectral slices (slower for lower-energy PL), most of the fast-component amplitude is present in a narrow spectral region. To systematically compare data for different samples, we hereafter bin all trPL to the blue of the time-integrated PL spectral maximum so as to yield characteristic ("blue-side") dynamics of the higher energy, prompt emission.

In Fig. 2, we display temporally resolved blue-side decay dynamics, normalized at late times, for multiple NC sizes at both 2.6 K and 80 K. For each sample, the low temperature dynamics become faster and biexponential in comparison to the slower single exponential decays recorded at high temperature. We summarize two general trends in Fig. 3: the blue-side becomes progressively longer-lived as the NC radius increases and the spectral shift associated with the fast decay feature yields a roughly constant value of ~25 meV irrespective of NC size (inset). The fast decay lifetime plotted vs NC radius squared exhibits a linear relationship. While such a trend has not been reported previously for a semiconductor NC composition, a comparable relation has been found in metal nanoparticles [18, 19] and is attributed to particle thermalization rates as dictated by interfacial and thermal diffusion [18-20].

Next, we probe the temperature dependence of the trPL collected for the 1.6-nm-radius sample. Fig. 4(a) shows that the amplitude of the fast decay feature remains unchanged between 2.6 and 10 K but that higher temperatures cause the fast-feature amplitude to decrease. To

highlight the evolution of the fast vs slow decay, Fig. 4(b) displays the temperature dependent ratio of instantaneous PL intensity binned from t = 0 to 5 ps divided by that from t = 200 to 205 ps for three CdSe NC sizes. Such ratios evolve with temperature similar to Boltzmann thermal partitioning with characteristic energies of 2.2, 1.5, and 1.0 (+/-0.1) meV for 1.2, 1.6, and 2.4-nm radii, respectively, in agreement with calculated lowest-energy acoustic phonon modes in CdSe NCs [16, 21].

In the respective contexts of wavepacket decoherence and intraband relaxation, Scholes [21-23] and Prezdho [24] recently proposed that acoustic phonons transiently mix dark and bright exciton states. In the picture presented by these authors, non-equilibrium acoustic phonons, generated in the current studies as a result of exciton intraband relaxation, mechanically distort the NCs and perturb the fine structure, which increases the oscillator strength of the lowest-energy dark exciton state. At the low temperatures examined in this work, the observed radiative recombination rate diminishes with time as these phonons leave the NCs. By contrast, for higher temperatures, there is a significant equilibrium population of acoustic phonons in the NCs. Furthermore, the increase of fast feature amplitude with decreasing temperature, explored in Fig. 4, follows the equilibrium thermal partition function describing NCs that lack acoustic phonon population. This relationship suggests that a single, lowest-energy equilibrium acoustic phonon is sufficient to preclude observation of the fast relaxation feature. Subsequent to acoustic phonon dissipation for low temperatures, the radiative rate decreases and LO phonon-assisted recombination dominates the ensemble PL spectrum, resulting in the size-independent red-shift. Acoustic phonon-induced mixing is also consistent with a noted lack of magnetic circular dichroism at early times following excitation [14] as well as the temperature dependent radiative recombination rates reported by Oron [16].

Next we focus on thermal transport estimates, first for a relatively large, 3-nm radius particle (for which bulk constants may be fairly accurate), and then as a function of NC size. Thermal transport models consider two regimes of heat dissipation: thermal diffusion controlled or interfacial conductivity controlled, each of which can dictate the timescale as well as the functional dependence on NC radius, R. We utilize the work of Ge et al [20] to estimate dissipation timescales specific to a CdSe NC suspended in an octadecane matrix initially at 10 K excited with 1-eV of photon energy in excess of the bandgap. Modeling the CdSe NC as a Debye solid (C follows T^3) reveals that the provided photon excess energy increases the temperature to ~16 K for a 3-nm radius particle (presented results were insensitive to the initial NC temperature at least within the range of 2.6 to 10 K).

For large thermal conductivity at the CdSe-alkane interface, thermal diffusion in the medium surrounding the NCs would dictate thermalization time and should follow $\tau_d=(C_p\rho_pR)^2/9C_m\rho_m\Lambda_m$ where, for the particle (p) and matrix (m), C is specific heat, ρ is density and Λ is linear thermal conductivity [utilized constants include $C_{p,initial}$(10 K)=0.012 J/gK, C_p(16 K)=0.061 J/gK, C_m(10 K)=0.011 J/gK, ρ_p=5.65 g/cm^3, ρ_m=0.777 g/cm^3, Λ_m=0.0015 J/cmKs]. For a 3-nm-radius NC, we estimate a diffusion cooling time under our experimental conditions of 90 ps (close to the interpolated 83 ps). Fig. 3 shows close agreement between diffusion-limited cooling times and experiment.

In the scenario of rapid diffusion, conductance of heat through the CdSe-alkane interface limits thermalization time and heat transport would obey $\tau_i=C_p\rho_pR/3G$, where G is an unknown interfacial thermal conductivity. Equating τ_i with the fitted data for a 3-nm radius NC then yields 4.1 MW/m^{2}K for G, which is two orders of magnitude smaller than the values obtained for metal nanoparticle dispersions [18-20]. However, as can be seen in Fig. 3, the functional dependence of

τ_i appears inconsistent with the measured lifetimes, suggesting that interface conductance does not limit thermal transport for the samples studied, and that the true value of G is significantly higher than this estimate.

In conclusion, we reveal a new size-dependent trend in the dynamics of CdSe NCs despite more than two decades of study in this material. We show that low temperature trPL exhibits faster sub-nanosecond decay for smaller NC size, attribute this trend to acoustic phonon dissipation, and denote consistency of the size-dependent decay times with a diffusion limited thermal transport process. The rapid emission is accompanied by bluer PL photons, which we attribute to acoustic phonon assisted relaxation. We ascribe a size-independent red-shift with time to reliance of dark exciton radiative recombination on LO-phonon assistance subsequent to acoustic phonon dissipation. Our findings impact the picture of truly Boltzmann-populated bright and dark excitons at elevated temperatures, suggesting that acoustic phonon derivative coupling provides optoelectronically relevant mixing of exciton fine structure character. Perhaps more importantly, we present a means to characterize heat flow rates involving semiconductor nanoparticles and provide evidence that thermal dissipation from the nanoparticles is determined by thermal diffusion in the surrounding material, rather than thermal impedance at the nanocrystal interface. These studies may offer means to intelligently design both low thermal conductivity nanomaterials for efficient thermoelectric power generation and high conductivity materials for stable device operation at elevated temperatures.

Use of the Center for Nanoscale Materials was supported by the U. S. Department of Energy, Office of Science, Office of Basic Energy Sciences, under Contract No. DE-AC02-06CH11357. This work was supported by the Non-equilibrium Energy Research Center (NERC) which is an Energy Frontier Research Center funded by the U.S. Department of Energy, Office

of Basic Energy Sciences under Award Number DE-SC0000989. RDS, SI, and DVT acknowledge support by the University of Chicago and the Department of Energy under section H.35 of U.S. Department of Energy Contract No. DE.AC02-06CHl1357 awarded to UChicago Argonne, LLC, operator of Argonne National Laboratory.

References

[1] P. O. Anikeeva *et al.*, Nano Letters **9**, 2532 (2009).

[2] A. P. Alivisatos, W. Gu, and C. Larabell, Ann. Rev. Biomed. Eng. **7**, 55 (2005).

[3] W. U. Huynh, J. J. Dittmer, and A. P. Alivisatos, Science **295**, 2425 (2002).

[4] K. F. Hsu *et al.*, Science **303**, 818 (2004).

[5] D. V. Talapin, and C. B. Murray, Science **310**, 86 (2005).

[6] V. I. Klimov, and D. W. McBranch, Phys. Rev. Lett. **80**, 4028 (1998).

[7] P. Guyot-Sionnest *et al.*, Phys. Rev. B **60**, R2181 (1999).

[8] E. Hendry *et al.*, Phys. Rev. Lett. **96**, 057408 (2006).

[9] M. G. Bawendi *et al.*, J. Chem. Phys. **96**, 946 (1992).

[10] M. Nirmal *et al.*, Phys. Rev. Lett. **75**, 3728 (1995).

[11] A. L. Efros *et al.*, Phys. Rev. B **54**, 4843 (1996).

[12] A. Franceschetti *et al.*, Physical Review B **60**, 1819 (1999).

[13] S. A. Crooker *et al.*, Appl. Phys. Lett. **82**, 2793 (2003).

[14] M. Furis *et al.*, J. Phys. Chem. B **109**, 15332 (2005).

[15] C. de Mello Donega, M. Bode, and A. Meijerink, Phys. Rev. B **74**, 085320 (2006).

[16] D. Oron *et al.*, Phys. Rev. Lett. **102**, 177402 (2009).

[17] A. I. Filin *et al.*, Phys. Rev. B **73**, 125322/` (2006).

[18] M. Hu, and G. V. Hartland, J. Phys. Chem. B **106**, 7029 (2002).

[19] O. M. Wilson *et al.*, Phys. Rev. B **66**, 224301 (2002).

[20] Z. Ge, D. G. Cahill, and P. V. Braun, J. Phys. Chem. B **108**, 18870 (2004).

[21] G. D. Scholes *et al.*, Nano Lett. **6**, 1765 (2006).

[22] V. M. Huxter *et al.*, Nano Lett. **9**, 405 (2008).

[23] V. M. Huxter, and G. D. Scholes, J. Chem. Phys. **132**, 10406/1 (2010).

[24] S. V. Kilina *et al.*, The Journal of Physical Chemistry C **111**, 4871 (2007).

FIGURE CAPTIONS

FIG. 1 (color online). (a) Temporally and spectrally-resolved single exciton PL from a 1.6-nm radius CdSe NC ensemble at 2.6 K and, (b), at 80 K. Here, lower sample temperature results in a faster emission feature as well as a spectral shift to lower energy with time. (c, d) Time-resolved spectra collected at the indicated temperatures and binned over the indicated time delays reveal a red-shift with increasing time at 2.6 K that is not observed at 80 K. Spectra are linearly offset for clarity. The black vertical lines indicate the peak emission amplitude of the 320 to 340 ps time-binned spectrum. (e, f) Spectrally-resolved PL dynamics become biexponential for shorter PL wavelength in the case of the lower sample temperature.

FIG. 2 (color online). "Blue-side" radiative recombination dynamics for CdSe samples with indicated radii generated for the higher energy half of the time-integrated PL spectrum at 2.6 K (blue lines) and 80 K (red lines). Traces were sclaed to overlap at long time. For every sample, the low temperature trPL data becomes biexponential. Also, the decay feature appearing at low temperature becomes increasingly faster with reduced NC radius. Note that the tick mark step size is constant (100 ps) for each data panel and that the measured time window is larger for larger NC size.

FIG. 3 (color online). The faster decay time derived from biexponetial fits of the trPL data in Fig. 2 (squares) exhibits a linear relationship with the NC radius squared (fitted black solid line). Calculations of diffusion limited (blue dashed line) and interfacial-conductance limited (grey dotted line, estimated for an interfacial conductance of 4.1 MW/m^2K) dissipation suggest that diffusion controls the measured decay times. The inset displays the energy difference between

early recombination and emission subsequent to the fast initial decay. The spectral shifts for multiple NC radii are fairly constant and comparable to the 25-meV LO phonon energy of bulk CdSe (solid red line). Recombination from higher lying states in the CdSe NC exciton fine structure is not apparent, since such emission would exhibit strong size-dependence corresponding to Δ_{db} values ranging from 2 to 17meV for the NC size-range probed.

FIG. 4 (color online). (a) Increasing sample temperature results in a decrease in amplitude of the fast dynamical component, here for a 1.6-nm radius CdSe NC sample. (b) The ratio of instantaneous PL intensities integrated from t = 0 to 5 ps (I_{early}) and from t = 200 to 205 ps (I_{late}) taken from dynamics such as those shown in 4(a) for three CdSe NC sizes suggests that Boltzmann populations of low-energy phonons in the NCs eliminates the fast relaxation feature for sufficiently high temperatures. Lines show appropriately scaled thermal partitioning of NCs lacking acoustic phonon excitation, as described in the text. Representative error bars are shown for the 1.30-nm radius NC sample.

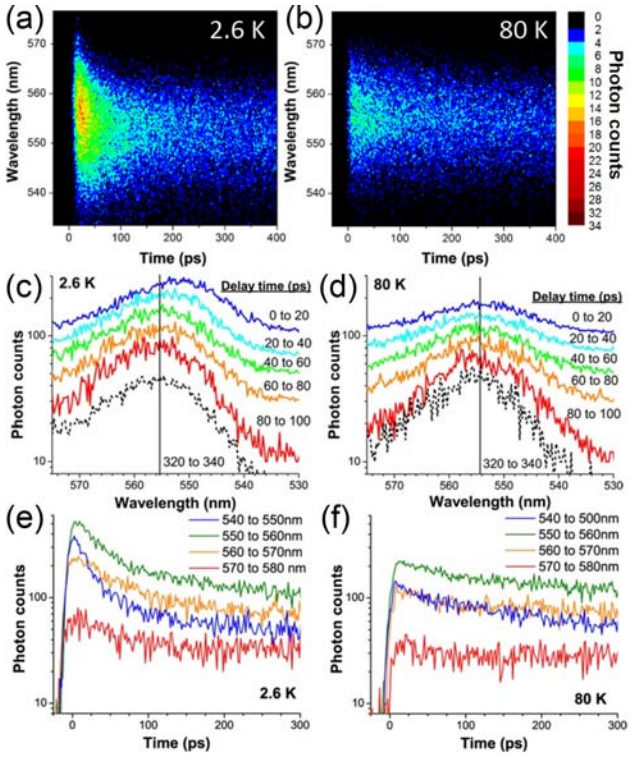
(a)
2.6 K
(b)
80 K
Wavelength (nm)
Time (ps)
Photon counts
(c)
2.6 K
(d)
80 K
Delay time (ps)
0 to 20
20 to 40
40 to 60
60 to 80
80 to 100
320 to 340
Photon counts
Wavelength (nm)
(e)
(f)
540 to 550nm
550 to 560nm
560 to 570nm
570 to 580 nm
540 to 500nm
550 to 560nm
560 to 570nm
570 to 580nm
Photon counts
Time (ps)
2.6 K
80 K

Figure 1

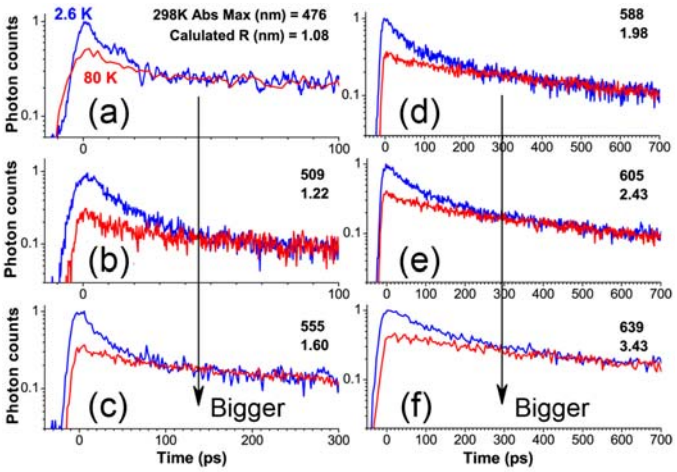
2.6 K
80 K
298K Abs Max (nm) = 476
Calulated R (nm) = 1.08
Photon counts
(a)
(b)
(c)
(d)
(e)
(f)
509
1.22
555
1.60
588
1.98
605
2.43
639
3.43
Bigger
Bigger
Time (ps)
Time (ps)

Figure 2

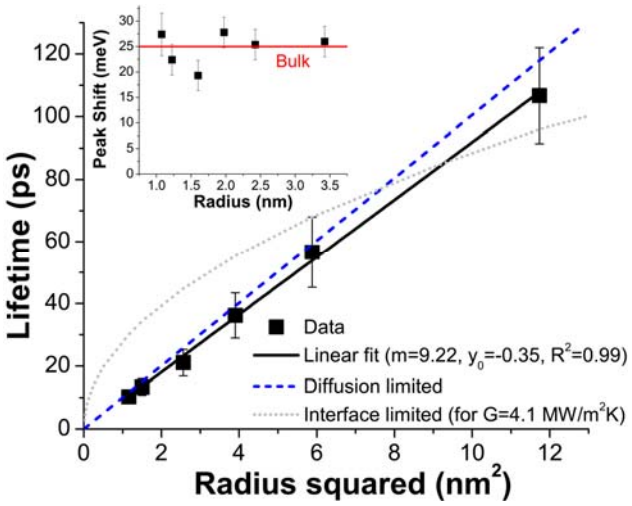
Lifetime (ps)
Radius squared (nm^2)
Peak Shift (meV)
Radius (nm)
Bulk
Data
Linear fit (m=9.22, y_0=-0.35, R^2=0.99)
Diffusion limited
Interface limited (for G=4.1 MW/m^{2}K)

Figure 3

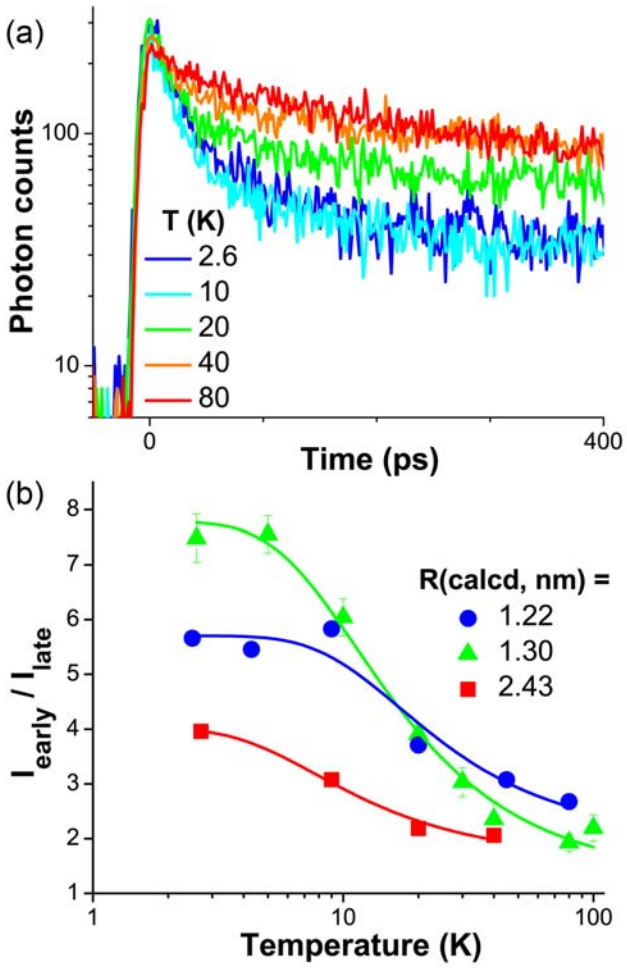
(a)
Photon counts
100
10
T (K)
2.6
10
20
40
80
0
400
Time (ps)
(b)
I_{early} / I_{late}
8
7
6
5
4
3
2
1
R(calcd, nm) =
1.22
1.30
2.43
1
10
100
Temperature (K)

Figure 4